Electronic Supporting Information

Enhancing the stability of inverted perovskite solar cells through Cu_2ZnSnS_4 nanoparticles hole transporting material

Elisa Fabbretti,[a] Amin Hasan Husien,[a] Rahul Patidar,[b] Karen Valadez-Villalobos,[b] James McGettrick,[b] Andreia Amighini Alerhush,[a] Ershad Parvazian,[b] Matthew L. Davies,[b] Trystan Watson,[b] Alessandro Minotto,[a] Giorgio Tseberlidis,[a] Adele Sassella,[a] Vanira Trifiletti[a] and Simona Binetti[a]*

[a] Department of Materials Science and Solar Energy Research Centre (MIB-SOLAR), University of Milano-Bicocca, Via Cozzi 55, 20126, Milan, Italy.

[b] SPECIFIC IKC, Faculty of Science and Engineering, Swansea University, Fabian way, Swansea, SA1 8EN, United Kingdom.

**Corresponding Author: vanira.trifiletti@unimib.it*

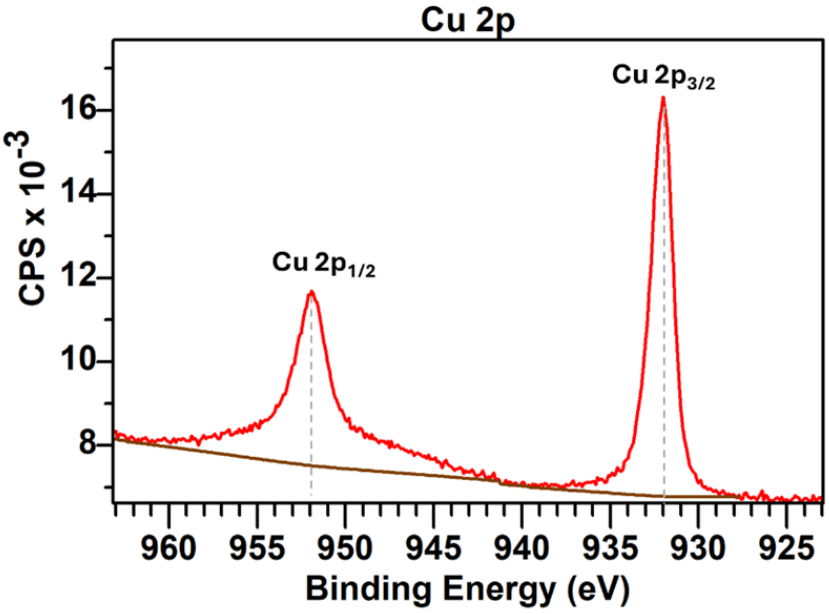

Figure S1 High-resolution XPS spectrum of Cu 2p of CZTS NPs powder.

Table S1 Positions and identifications of the main peaks in XPS spectra for CZTS NPs film annealed at 350°C, 300°C and 250°C.

T (°C)	Cu 2p (eV)	Zn 2p (eV)	Sn 3d (eV)	S 2p (eV) (Sulfide)	Cu satellite (eV)	Zn Auger LMM (eV)	S 2p (eV) (Sulfate)	N 1s	C 1s
350	$2p_{3/2}$: 932.9 $2p_{1/2}$: 952.7	$2p_{3/2}$: 1022.2 $2p_{1/2}$: 1045.3	$3d_{5/2}$: 486.9 $3d_{3/2}$: 495.3	$2p_{3/2}$: 161.5 $2p_{1/2}$: 162.6	940.0 - 945.0 962.7	499.6	$2p_{3/2}$: 168.9 $2p_{1/2}$: 170.0	A: 400.2 QA: 402.1	C-C: 284.8 C-O-C: 286.4 C-N, O-C=O: 288.6
300	$2p_{3/2}$: 932.8 $2p_{1/2}$: 952.6	$2p_{3/2}$: 1022.4 $2p_{1/2}$: 1045.4	$3d_{5/2}$: 487.1 $3d_{3/2}$: 495.5	$2p_{3/2}$: 161.4 $2p_{1/2}$: 162.6	940.8 - 944.3 962.9	499.9	$2p_{3/2}$: 169.0 $2p_{1/2}$: 170.2	A: 400.0 QA: 401.9	C-C: 284.8 C-O-C: 286.4 C-N, O-C=O: 288.6
250	$2p_{3/2}$: 932.2 $2p_{1/2}$: 952.1	$2p_{3/2}$: 1022.3 $2p_{1/2}$: 1045.4	$3d_{5/2}$: 487.0 $3d_{3/2}$: 495.4	$2p_{3/2}$: 161.4 $2p_{1/2}$: 162.5	- -	499.7	$2p_{3/2}$: 169.0 $2p_{1/2}$: 170.1	A: 400.2 QA: 402.0	C-C: 284.8 C-O-C: 286.4 C-N, O-C=O: 288.6

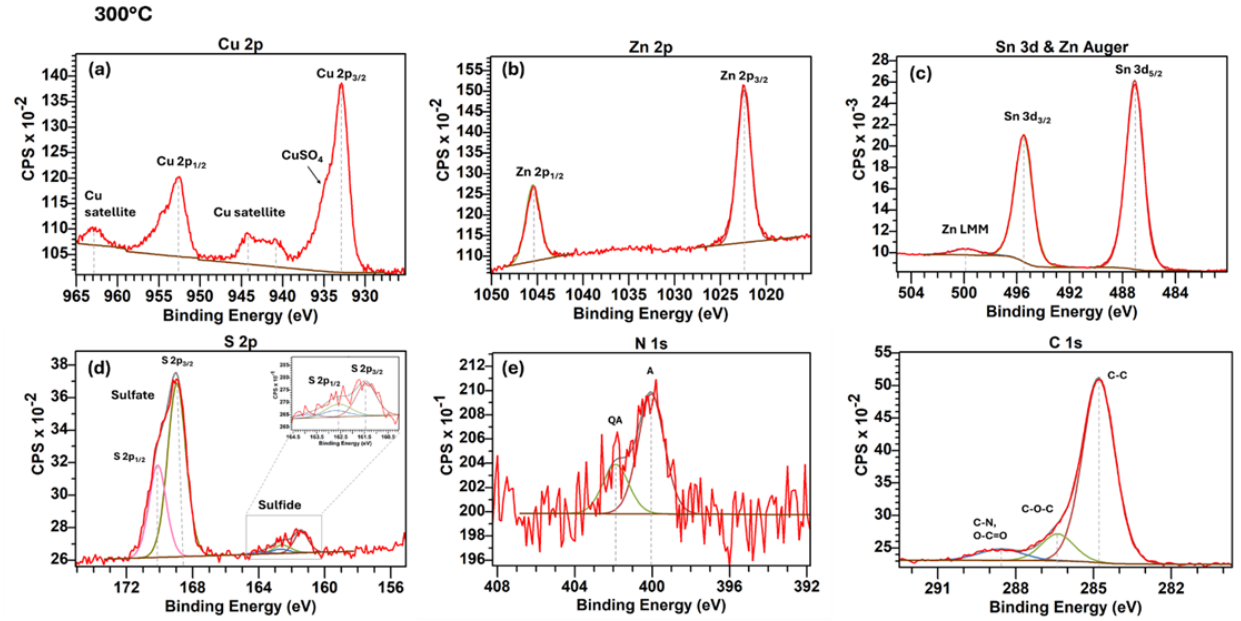

Figure S2 High-resolution XPS spectra for (a) Cu 2p, (b) Zn 2p, (c) Sn 3d and (d) S 2p components of CZTS NPs film annealed at 300 °C, and XPS spectra of impurities containing (f) N 1s and (e) C 1s.

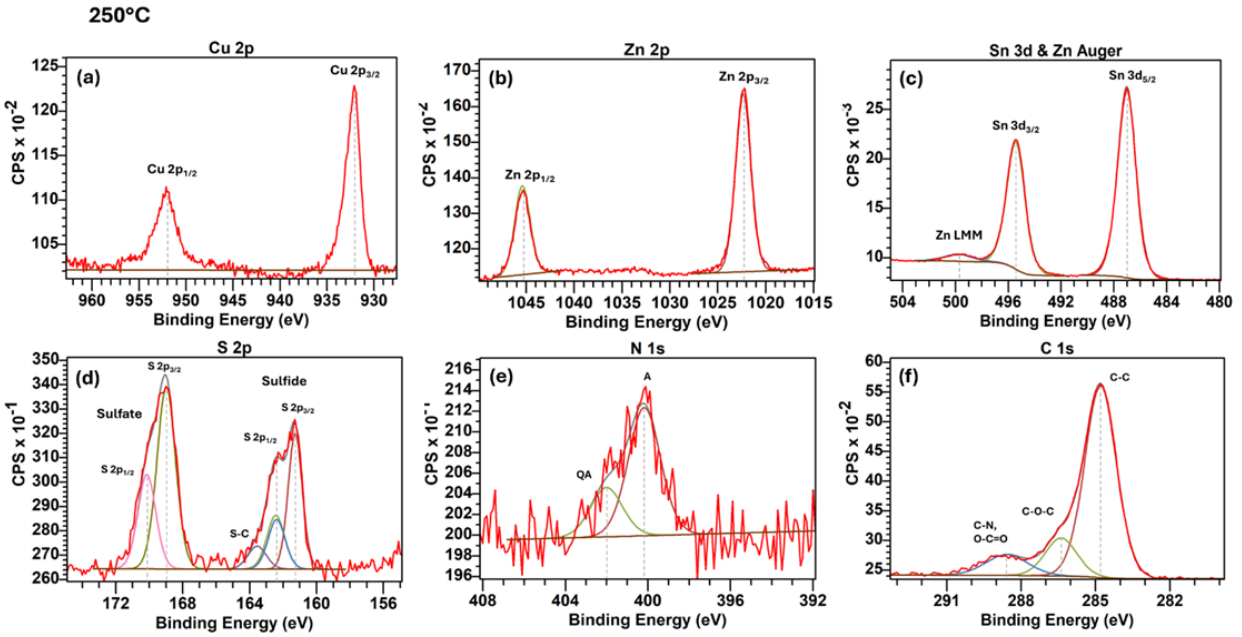

Figure S3 High-resolution XPS spectra for (a) Cu 2p, (b) Zn 2p, (c) Sn 3d and (d) S 2p components of CZTS NPs film annealed at 250 °C, and XPS spectra of impurities containing (f) N 1s and (e) C 1s.

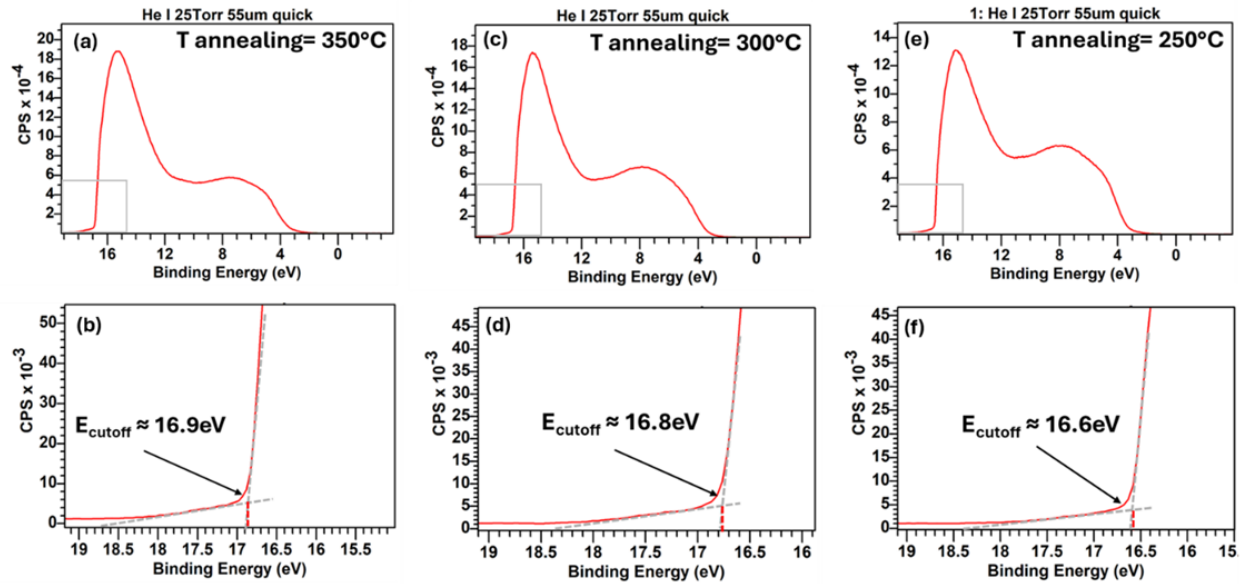

Figure S4 UPS spectrum for CZTS NPs films annealed at (a) 350 °C, (c) 300 °C and (e) 250 °C, and (b), (d), (f) the respectively cutoff energy E_{cutoff} extrapolated from the high binding energy spectra side. All the spectra were obtained at excitation photon energy ~ 21.2 eV.

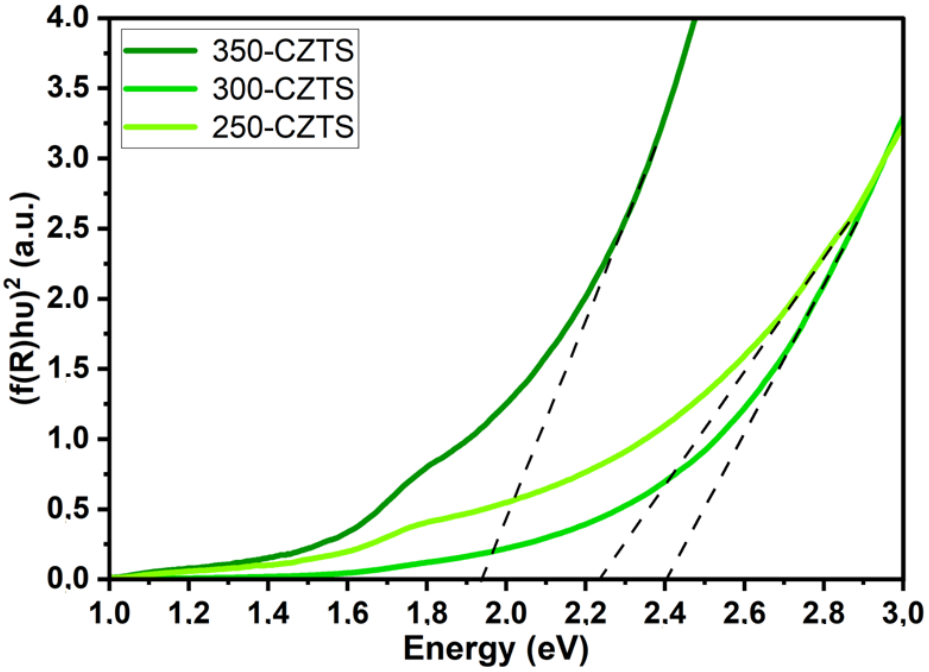

Figure S5 Kubelka-Munk plot for the CZTS layers annealed at 250°C, 300°C and 350°C.

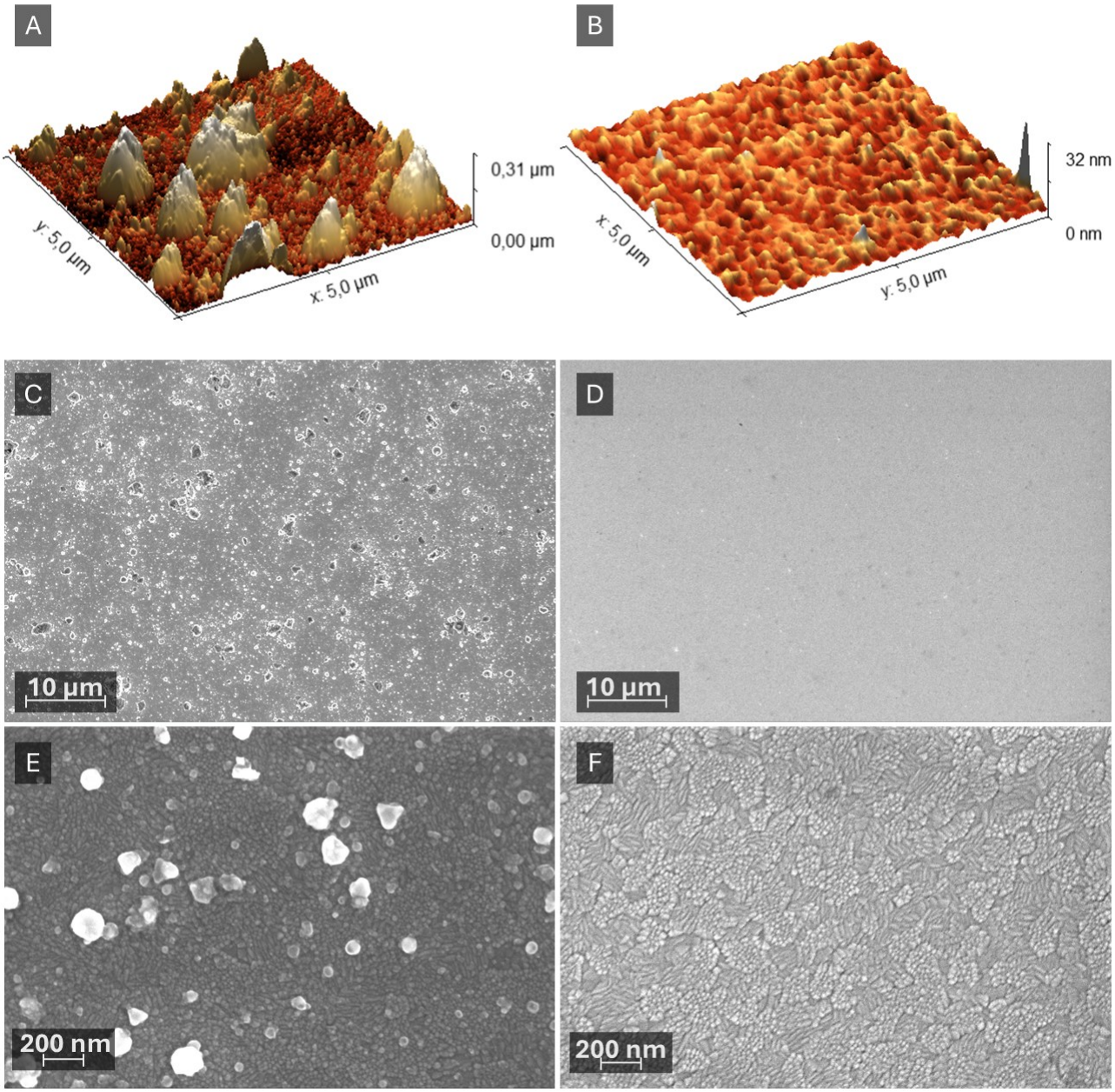

Figure S6 Comparison of surface morphology for CZTS NPs and MeO-2PACz (SAM) layers. (A, C, E) AFM mapping over a 5 µm x 5 µm scale and SEM images (20 µm and 200 nm scales, respectively) of the CZTS NPs layer deposited on ITO. (B, D, F) Corresponding AFM map and SEM images for the MeO-2PACz (SAM) layer.

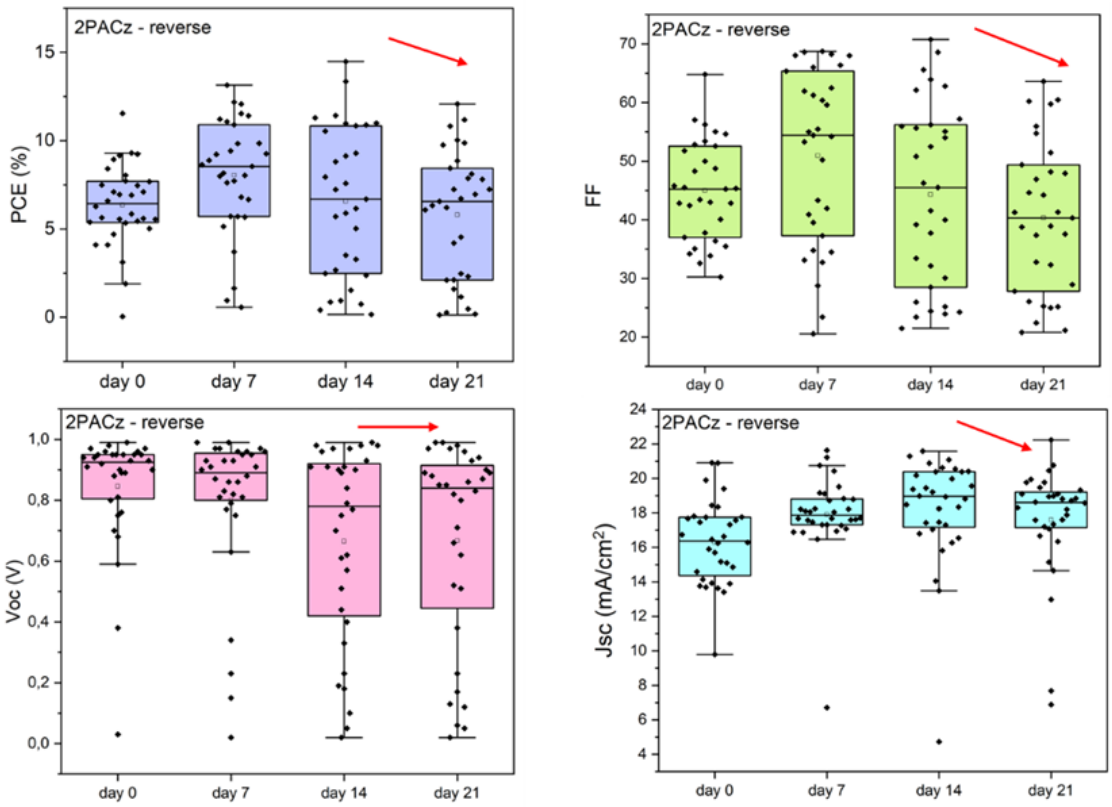

Figure S7 Box chart indicating the trend of 32 MeO-2PACz-based control devices' performances over several days.

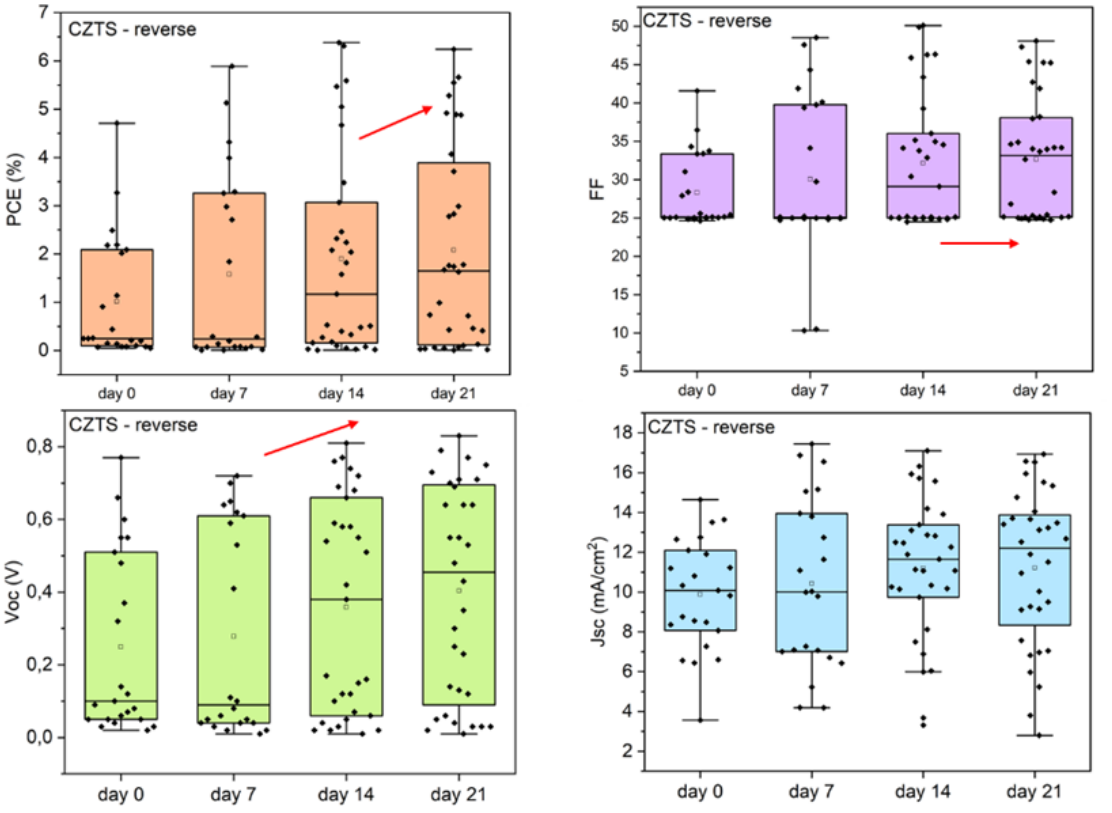

Figure S8 Box chart indicates 32 CZTS-based devices' performance trends over several days.

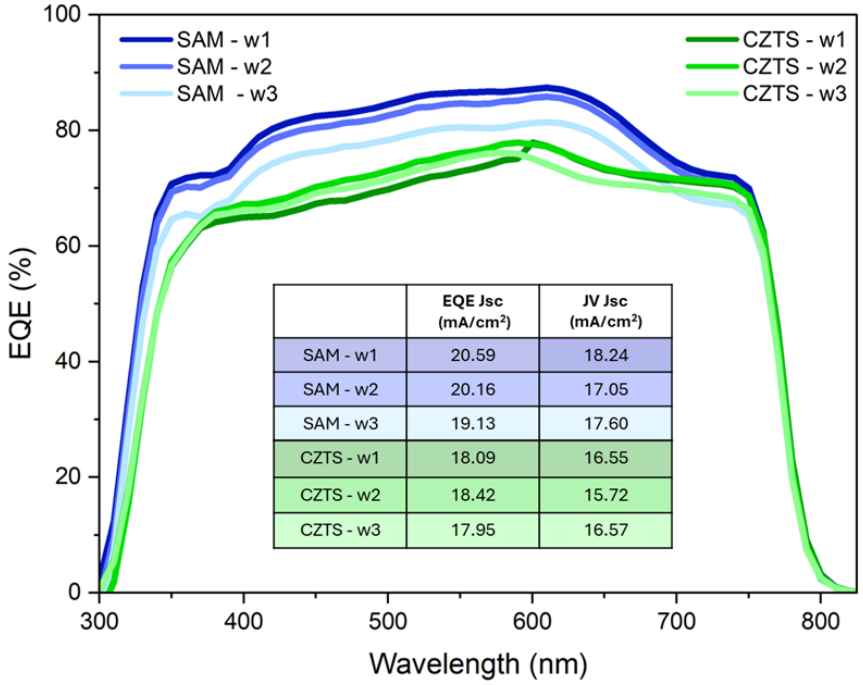

Figure S9 EQE spectra of the CZTS-based and the control devices obtained over different weeks.

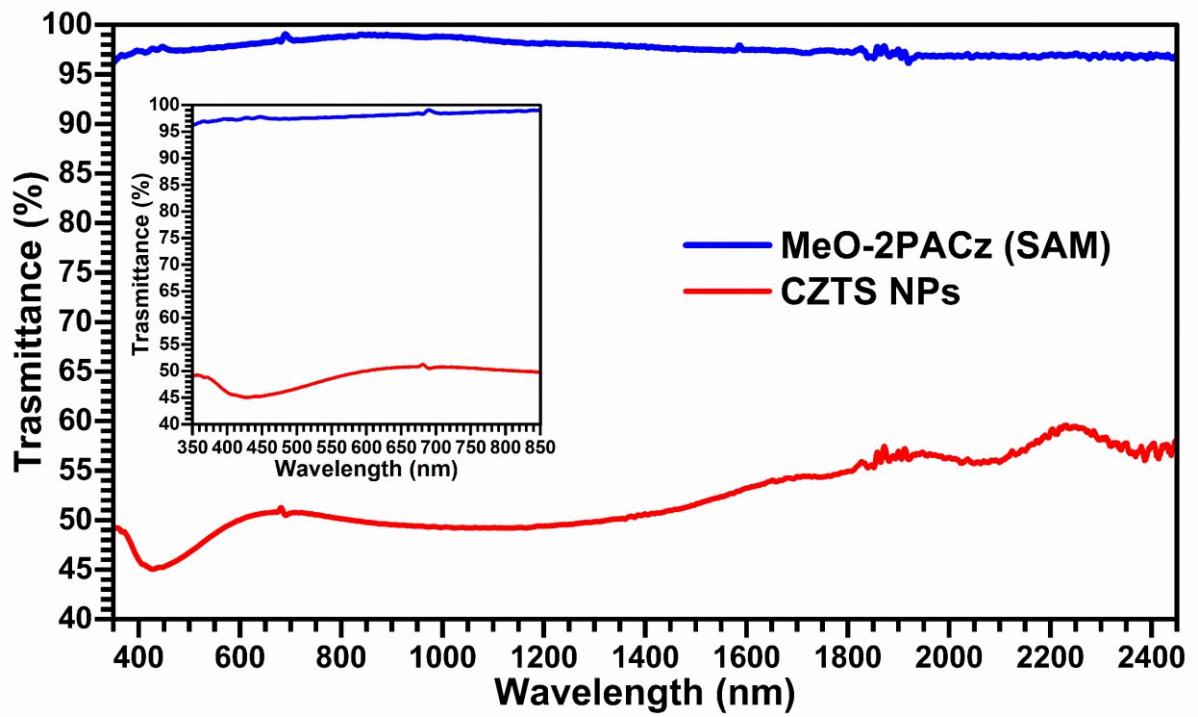

Figure S10 Transmittance spectra of CZTS NPs and MeO-2PACz (SAM) layers (inset: zoom on the visible region of the spectra).

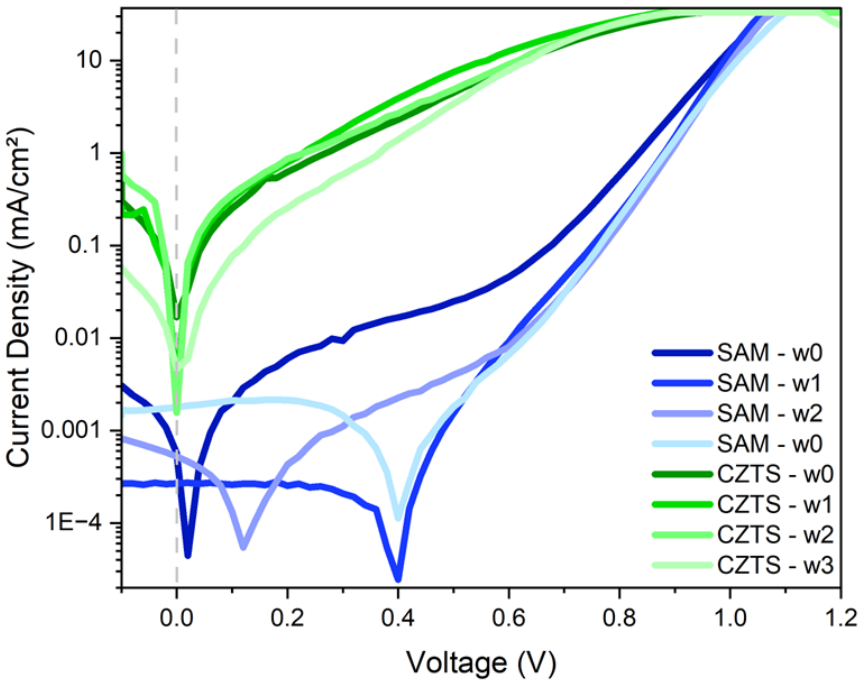

Figure S11 JV curves under dark conditions of the CZTS-based and the control devices measured over days to investigate the stability of both the perovskite solar cells.